Heliyon 9 (2023) e15956

Contents lists available at ScienceDirect

Heliyon

journal homepage: www.cell.com/heliyon

Research article

Methodology for assessing pipeline failure probability due to a debris flow in the near field

Su Song [a], Weizhuo Hua [b], Xiaolong Luo [c], Ana Maria Cruz [d,*]

[a] Department of Urban Management, Graduate School of Engineering, Kyoto University, Kyoto, 615-8540, Japan
[b] School of Energy and Power Engineering, Xi'an Jiaotong University, Xi'an, Shaanxi, 710000, China
[c] Institute for Disaster Management and Reconstruction, Sichuan University, Chengdu, Sichuan, 610207, China
[d] Disaster Prevention Research Institute, Kyoto University, Kyoto, 611-0011, Japan

ARTICLE INFO

Keywords:
Transmission pipeline
Model integration
Pipeline failure probability
Debris flow
Cascade process

ABSTRACT

Aboveground transmission oil pipelines can cross debris flow-prone areas. Currently, there are no available methodologies to assess pipeline failure status with the different pipeline arrangements (location, direction, and segment lengths) and different operating conditions. For solving the research gap, this study proposes a novel methodology to simulate the cascade processes of debris flow propagation, the impact of debris flow on pipelines, and pipeline failure. With consideration of different pipeline arrangement and operating conditions. We introduce the polar coordinate system to set up locations and directions scenarios for the first time. Also, we use the 3-D debris flow simulation model (DebrisInterMixing solver in OpenFOAM) coupled with a modified pipeline mechanical model considering operating conditions for the first time. The proposed methodology shows the different trends of pipeline failure probability with the increase of pipeline segment length for the different pipeline locations and directions. The result shows, for the pipelines of 30° the tensile stress has a more moderate increase rate with the increase of pipeline segment length, and the pipeline failure probability keeps 0 at the 5-m location. At 5 m and 15 m locations, the failure probabilities of the pipelines of 60° and 90° start to increase when the segment length is 13–14 m, while for other pipelines the segment length is 17–19 m. The findings of this study can support the decisions of government authorities, stakeholders, and operators for risk assessment, prioritization of hazard mitigation measures and emergency planning, or concerning decisions regarding pipeline siting during the design, routing, construction, operation, and maintenance stage.

1. Introduction

Natural hazard events can trigger severe consequences in the chemical and process industries, such as equipment damage and loss of containment, which can cause toxic dispersion, fire explosions, and environmental contamination. In the literature [1,2], these types of events are referred to as Natech events. An example of a Natech event is one that occurred in Montecito, California, USA in 2018, where debris flow caused by heavy rainfall was initiated from an area incinerated by the Thomas Fire. Consequently, a high-pressure transmission gas pipeline was affected, which resulted in gas leak and a severe explosion that destroyed numerous houses [3]. In this case, the hazardous debris flow is known as a geo-hazard. Girgin and Krausmann analyzed pipeline accident data obtained from the

* Corresponding author.
E-mail address: cruznaranjo.anamaria.2u@kyoto-u.ac.jp (A.M. Cruz).

https://doi.org/10.1016/j.heliyon.2023.e15956
Received 1 October 2022; Received in revised form 17 April 2023; Accepted 27 April 2023
Available online 4 May 2023

PHMSA (Pipeline and Hazardous Materials Safety Administration)and NRC (U.S. National Response Center) [4]. The report showed that geological hazards constituted the majority of Natech accidents (i.e., 37% of all transportation pipeline accidents). Therefore, during the design, construction, and operation of pipelines, one must assess the geo-hazard risk of pipelines, particularly when significant engineering, environmental, and socioeconomic issues are involved [5]. The geo-hazard risk assessment of pipelines allows us to identify the threat of geo-hazards and facilitates in pipeline route selection [6,7].

Analyzing the interaction between geo-hazards and pipelines is the main component in geo-hazard risk assessment and an important aspect in pipeline integrity management. A typical scenario associated with this interaction is a pipeline spanning a hazardous area. Owing to land limitations or economic and political reasons, a pipeline that span hazardous areas is exposed to geo-hazards. The interaction between these pipelines and the associated geo-hazards must be analyzed during pipeline design and routing. A landslide, as a typical geo-hazard, refers to the movement of rocks, earth, or debris down a sloped land section. To address this potential hazard, local authorities and stakeholders must consider the appropriate methods when arranging pipelines across possible hazardous areas. For example, pipelines can be arranged along the direction where landslides tend to occur instead of arranging them along the surface alignment. One of the landslide types features shallow debris flows, rapidly moving landslides, and a slurry of fine (sand, silt, and clay) and coarse materials (cobbles and boulders) mixed with water [8]. Hence, the debris flows are similar to flash floods and can occur abruptly. When the drainage channel eventually becomes less steep, the liquid mass distributes widely and decelerates in terms of its movement, thus contributing to the formation of a debris fan or mudflow deposit. Owing to this debris flow scenario, pipeline managers must devise appropriate methods for routing pipelines across areas that may be affected by debris flows.

Previously, researchers have primarily focused on the safety of pipelines. For example, Wu Ying proposed finite element analysis on the mechanical behavior of semi-exposed and buried pipelines subjected to debris flows [9,10]. M. Hongqiang et al. use the experiment and simulation to investigate strain characteristics of the buried natural gas pipeline under longitudinal landslide debris flow [11]. These studies forced on the pipeline material characteristic during the impact of the debris flow. As the relationship between debris flow and pipeline belongs to the solid and fluid. H Pourziaei Araban proposed fin shape and arrangement effects on entropy generation and hybrid fluid-solid-fluid heat transfer [12]. M. M. Peiravi investigated the effects of different arrangements of three-dimensional fibers on polymer matrix composite thermal conductivity under heat flux boundary conditions [13]. Javad Alinejad et al. investigated the effect of different spaces and objects on the heat transfer with different types of fluid. These studies clarified the importance of calculation space and objects [14–17]. Thus, considering the impact of debris flow on the pipeline, not only focusing on the pipeline failure with the consideration of unique impact scenario but also focusing on more scenarios of different pipeline alignments is needed based on the practice of engineering. And the limitation due to calculation space and pipeline structure cannot be ignored.

As the statement above, in practice, one must consider aspects other than pipeline safety. During the decision-making process, in addition to ensuring the safety of pipelines, one must consider (i) the conditions in which workers can perform their duties with low risks of injury, (ii) approaches to reduce construction costs, and (iii) the effects of operating conditions. Hence, government authorities and stakeholders are attempting to ensure pipeline safety during its construction and operation, ensure the safety of workers, and reduce construction and maintenance costs.

Different pipeline arrangements, which involve different pipeline locations (routes), directions, and pipeline segment lengths, result in different costs and difficulties in pipeline construction. Different operating conditions can generate different pipeline stress. Furthermore, under the same debris flow, a load of debris flow on the pipeline will be different and thus results in different pipeline statuses (safe or fail). These comprehensive information related to pipelines needs to be obtained. However, there is no assessment approach available to meet this requirement. Hence, this study proposed a methodology to integrate pipeline factors (arrangements and operating conditions) to assess the pipeline failure status. Government authorities, stakeholders, and operators must compare all possible pipeline arrangements with operating conditions, then select the best option relied on the corresponding pipeline status.

Currently, this assessment is hindered by several challenges. First, during construction and routing, terrain analysis is used primarily for pipeline geo-hazard risk analysis [7]. However, terrain analysis does not allow one to assess loads on pipelines accurately, particularly in the near field. Moreover, although changing the pipeline arrangement has been applied so that the pipeline does not span areas susceptible to ground movement [18], there is no approach to take the factors (Segment length, location, and direction) of pipeline arrangement into account comprehensively. Moreover, during the operation of a pipeline, its operating conditions affect its vulnerability to hazards, including debris flow hazards. In reality, operational conditions often exhibit uncertainties, thus resulting in uncertain pipeline vulnerabilities [19]. However, a pipeline vulnerability model for debris flow that can assess pipeline failure probability has not been developed.

In this study, we first determine an approach to assess the load of debris flow on a pipeline. As mentioned above, basic information is obtained via terrain analysis. The key to solving this problem is to identify the connection between the information and the load of the debris flow. Notably, loads of debris flow occur in the propagation stage, and debris-flow run-out must be predicted. Considering that the information may include the potential source of debris flow (location and depth), it can be used in a debris flow numerical simulation to predict the propagation of debris flow. Furthermore, the prediction results can be used to calculate the loads on the pipeline. Next, the pipeline arrangement is to be considered. Considering the abovementioned approach, a pipeline can be regarded as a straight line crossing an area, and the key to solving this problem is to devise a method that allows any line to be specified easily. Thus, the polar coordinator system can be introduced to consider all possible scenarios as one point and a line can be easily referred to debris flow source. Using this system, all points on a line can be used as the origin of the specified line, and all scenarios can be considered by adjusting the angle between the line and the specified line. Moreover, because of the operation conditions, the pipeline failure probability can be obtained provided that the relationship among the operation conditions, loads on pipelines, and pipeline strength is determined, even if the pipeline vulnerability model of debris flow is not available. In this regard, a simplified pipeline mechanical model [20], which has been proven successful in assessing the effect of additional loads, can be used. Ahammed et al.

discussed pipeline stress behaviors caused by the operation conditions of oil pipelines [19]. Although loads of debris flow or loads of other hazards were not considered in that study, the authors were able to introduce relationship functions established between the generated stress and operation conditions into the pipeline mechanical model.

This study is aiming to supply a guide to show when facing a potential debris flow, what factors should be considered, and how to predict consequences. This study adopts some simplification operations by assuming the initial scenario of debris flow, calculation space, and pipeline construction. In the present study, a three-dimensional (3D) debris flow simulation and a modified pipeline failure model are used to develop a methodology to assess pipeline failure probability by considering the pipeline arrangements and operation conditions. The DebrisInterMixing solver is used to conduct the 3D simulation and to calculate the loads on pipelines over time [21, 22]. In the simulation, pipeline arrangements are established by transferring them to the surface grid structure in OpenFOAM. The loads are used as inputs to the modified pipeline failure model. By using this model and considering the uncertainty of the operating conditions, the pipeline failure probability is obtained by sampling the value of operating conditions. The developed methodology can consider multiple aspects that affect pipeline stability, thus allowing local authorities, pipeline stakeholders, and operators to decide reasonably. In addition, the feasibility of this model is clarified. This study provides a methodology that can guide pipeline designers in decision-making, as well as the associated data and approach. The case study presented herein is based on assumptions for simplifying complex data, which are beneficial to the proposed methodology.

The remainder of this paper is organized as follows: Section 2 describes the workflow of the proposed methodology and the input and output data used. Section 3 introduces the basic assumptions introduced for the case study as well as provides the results and discussion. Section 4 presents the conclusion, limitations, and outlook.

2. Proposed methodology

A flowchart presented in Fig. 1 shows the proposed methodology for assessing the probability of transportation pipeline failure due to debris flow. This methodology primarily includes five steps: clarifying the schematization of debris flow and pipeline, as well as data acquisition (Step 1); preprocessing of debris flow simulation, which primarily includes setting the pipeline arrangement, other parameters, and boundary conditions (Step 2); performing calculations for debris flow simulation (Step 3); post-processing debris flow simulation for calculating loads on the pipeline (Step 4); and calculating the pipeline failure probability (Step 5).

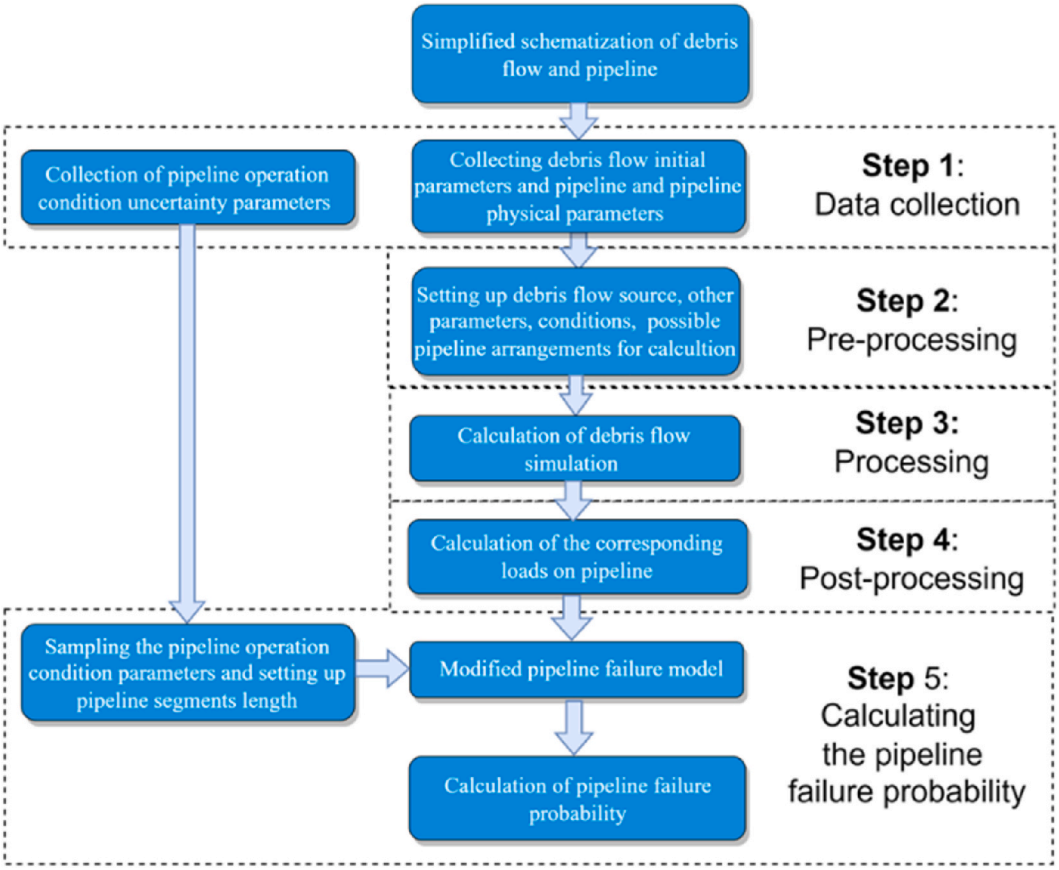

Fig. 1. Methodology.

2.1. Schematization

The schematization of the debris flow and pipeline, which is related to the debris flow source and pipeline alignment, is clarified in this section. A schematic illustration of the interaction between the debris flow and pipeline is shown in Fig. 2(a) [19]. The shapes, sizes, locations of the sources and the initial pipeline parameters should be determined based on the initial conditions. In addition, Fig. 2(b) shows the force distribution of pipeline including external load and pipeline stress [20]. The external force includes a drag force and a lift or buoyancy force mainly due to the debris flow. The pipeline stress is mainly generated along the axial and circumferential directions due to the operation condition (internal pressure and temperature). The pipeline failure determination and the above-mentioned force calculation are explained below.

2.2. Solver for debris flow simulation

In this study, DebrisInterMixing-2.3, which is a finite volume solver for 3-D debris flow simulations [22,23], was used. Von Boetticher et al. specified debris flow as a type of incompressible flow and used the volume-of-fluid approach for three phases in a single cell-averaged Navier–Stokes equation. The simulation was performed by performing coding in OpenFOAM [21]. Von Boetticher et al. validated the model via a physical experiment. Because the aim of the study was to devise an approach, the authors used the same physical parameters as those for debris flow simulation [22].

2.3. Preprocessing for debris flow simulation

Because of the solver requirements, the preprocessing for the simulation required mesh generation and the setting of debris flow fields. This entails generating 3D print files for the debris flow source and pipeline surface, creating a spatial mesh for the calculation space, and setting the boundary conditions for the simulation. These aspects are described comprehensively in the following subsections.

2.3.1. Approach for setting pipeline alignment

The pipeline alignment determines the method by which the pipeline spans debris flow areas. In this study, the pipeline is set as an aboveground transmission oil pipeline instead of the buried pipeline as buried pipelines are not impacted because of protection by the surrounding soil normally. However, this study is also adapted to buried pipelines as follows. Besides the aboveground pipeline can be constructed in some areas, such as in Colombian, in certain situations, debris flow impacting pipelines can occur during the life cycle of a buried pipeline, such as the construction and design stages, the oil pipeline must be placed on the surface of the earth based on the appropriate route. For example, excavation and landfilling can be performed only after a few weeks or months. In addition, during the operation stage, the soil layer above the pipeline can be eroded by rivers or other types of ground movement. In these situations, the pipelines can be exposed to debris flow.

In this study, the pipeline is assumed lain out along the surface of the earth as shown in Fig. 3. The pipeline alignments can be determined by the determination of pipeline routes x–y plane. In addition, Fig. 3 also shows the calculation space and boundary. In this calculation space, two lines are assumed. The dash line presents any possible line in the space and another line is the specified line mentioned above. The specified line presents a pipeline and is determined by the origin (O point) and angle (α). The origin is obtained on the dash line and the specified line (pipeline route) can be determined by setting the angle. In this study, for clarifying the location of the pipeline route, the pipeline serial number is set as 'pipeline (O, α)'. For example, pipeline (A, 30°) presents a pipeline which is of the origin A point and 30° angle. To avoid overlapping scenarios, all possible scenarios were established based on the origin from the dash line that spanned this area, as well as angles from 0° to 180°. In this study, the debris flow source is located at the space boundary and the dash line is assumed to site the center of the calculation space and cross the debris flow source. For clarifying the position of origin, the distance D represents the distance from the origin to the space boundary on the plane.

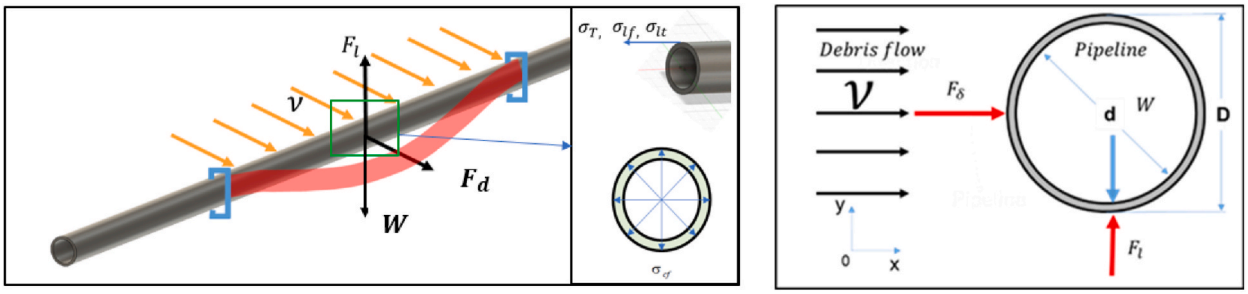

Fig. 2. Schematic illustration showing interaction between debris flow and pipeline.

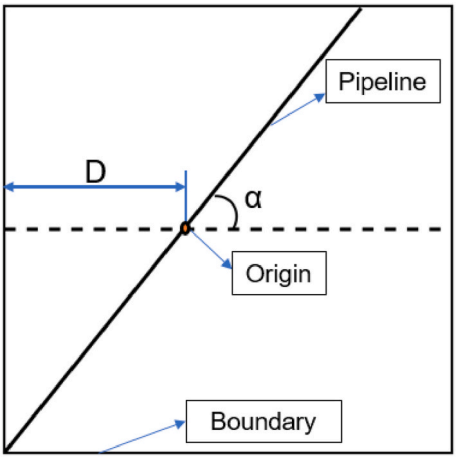

Fig. 3. Schematic illustration of the pipeline route.

2.3.2. *Mesh generation, field, and boundary setting*

To perform the debris flow simulation, the mesh and setting of the field for the debris flow in the calculation space are required. To obtain the loads on the pipeline, a mesh needs to be generated in the calculating space and a surface mesh of the pipeline need to be generated and inserted into the generated calculating space mesh. For the setting of the field, the initial conditions of the debris flow and the other space need to be set. Before these pre-processing operations, the 3-D printing files of pipeline and debris flow sources are required, which includes the sizes and spatial information.

In this study, 3-D files were drawn using the AutoFusion 3-D drawing software. A mesh generator tool known as blockMesh was used to construct the space mesh in OpenFOAM, which included an internal mesh and a boundary mesh, and another mesh generator tool known as snappyHexMesh was used to generate the pipeline surface mesh using 3-D printing files of the pipeline. The setFields tool was used to set the enveloped space as the source of debris flow using the 3-D printing files of the debris flow source. Subsequently, the initial conditions for the debris flow simulation were specified. For each pipeline scenario, a one-time processing was required. For the boundary conditions, the surface of the slope, the plane, and the pipeline were set as wall elements, and other boundaries were set as outflow elements, which implies the absence of objects to stop debris flow outflow.

2.4. *Post-processing and external load calculation*

ParaView, which is an open-source, multi-platform data analysis and visualization application, was used in this study to perform post-processing and load calculation. Based on Fig. 1, a debris flow can cause lift and drag forces on the pipeline surface. To obtain the value of these forces, post-processing was conducted in ParaView based on time-step results. As the lift and drag forces are caused by the pressure of the debris flow on the pipeline surface, one must obtain the pressure values in the cells of the pipeline surface mesh. Fig. 4 shows the workflow of the force calculations. First, the cells of the pipeline surface can be extracted by performing the extract-block and extract-surface operations in ParaView. Subsequently, the normal stresses of these cells can be obtained using the

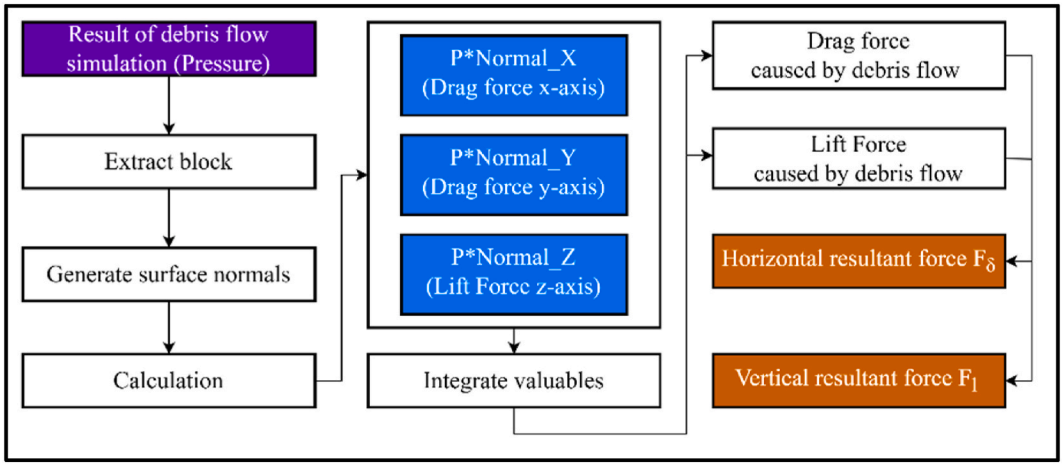

Fig. 4. Calculation of resultant force.

"Calculator" tool in ParaView. Finally, the drag and lift forces exerted on the pipeline can be determined by integrating the values obtained.

It should be noted that when calculating the vertical resultant force two scenarios need to be considered. When the gravitational force due to the weight of the pipeline and oil is greater than the buoyancy force, the vertical resultant external force is equal to 0 N. However, when the gravitational force is lower than the buoyancy force, the vertical resultant external force is equal to the value of the lift force (F_l) minus the gravitational force (W).

2.5. Pipeline stress due to operation conditions

Ahammed et al., 1997 explained the relationship between stress and operating conditions (internal pressure and temperature). The internal pressure (p) causes longitudinal and circumferential stresses, which shows in Eqs. (2) and (3). And a temperature change $\Delta\delta$ can cause longitudinal stress, which shows in Eq. (1).

$$\sigma_{lt} = EC\Delta\delta[10] \tag{1}$$

$$\sigma_{lf} = \frac{vpr}{t} \tag{2}$$

$$\sigma_{cf} = \frac{pr}{t} \tag{3}$$

Here, σ_{lt} is the longitudinal stress due to temperature , σ_{lf} the longitudinal stress due to internal pressure, σ_{cf} the circumferential stress due to internal pressure, E is the modulus of elasticity, ν is the Poisson's ratio, r is the pipeline radius, and C is the coefficient. In reality, the internal pressure and temperature change over time.

2.6. Pipeline failure probability due to uncertain operation conditions

A pipeline mechanical model that can determine the pipeline failure and probability by considering the uncertain operating conditions is required. A pipeline can be considered a linear construction and a pipeline structure behave as a beam. Thus, a beam mechanical model was used in this study. Owing to the super-stationary problems of the system, the displacement method was used to determine the solutions of the failure mechanical model. Fig. 5 shows a schematic illustration of a debris flow impacting a pipeline, where L_s is the segment length, and L_i is the impacted length. When the segment length is larger than the impacted length, the load is a total uniform load; otherwise, the loads on the pipeline are partial. Eqs. (4) and (5) are the corresponding calculation approach to the binding moment M. Here, σ_t denotes the stress along the direction of the pipeline axis. To calculate the equivalent stress, Eqs. (8) and (9) by Ahammed et al., 1997 which are also used for determining pipeline failure, can be used. In this study, the resultant stress in the pipeline direction was caused by the internal pressure, temperature change, and bending stress due to the impact of debris flow. The resultant stress along the pipeline direction can be calculated using Eq. (7).

Because of these functions, one set of input data can yield one result. In reality, the operating conditions often reflect one type of statistical distribution. A random resampling was performed in this study to obtain data pertaining to the operating conditions, which were used as the input data. Equations (4)–(7) can be used to obtain the binding moment M, second moment of area I, and tensile stress

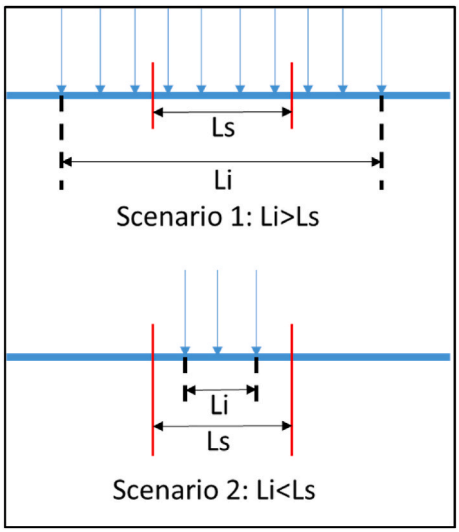

Fig. 5. Schematic illustration of segment length and impacted length.

σ_t.

$$M = \frac{qLiLs^2}{24} * \left[3 - \frac{li}{Ls} + \left(\frac{li}{Ls}\right)^2\right] \text{ Scenario 1} \left[26\right] \tag{4}$$

$$M = \frac{qLs^2}{12} \text{ Scenario 2} \tag{5}$$

$$I = \pi D^4 \left(1 - \frac{d^4}{D^4}\right) \Big/ 64 \tag{6}$$

$$\text{Tensile stress} : \sigma_t = M * D / (2I) \tag{7}$$

where L_s is the segment length, and L_i is the impacted length where q is the drag force per meter, D the external diameter, and d the internal diameter. Here, if the equivalent stress σ_{eq} is equal to or greater than the allowable yield stress of the material of the pipeline σ_a, then one may assume that the pipeline has failed. Longitudinal and circumferential stresses were generated owing to the internal pressure and temperature change. Table 1 lists the parameters mentioned above. Equation (9) shows the criterion for determining pipeline failure.

$$\sigma_l = \sigma_{lf} + \sigma_{lt} + \sigma_t \tag{8}$$

$$\sigma_c^2 - \sigma_c\sigma_l + \sigma_l^2 > \sigma_a^2 \quad \left(\sigma_{eq}^2 > \sigma_a^2\right) \tag{9}$$

where σ_l, σ_c is the resultant longitudinal and circumferential stress in Eq. (8), σ_a is the allowable yield stress, which is equal to 0.6* σ_y (yield stress) based on the GB50253-2014 [24]. The above functions are coded into Matlab. Because the pipeline operating condition parameters follow the log distribution [10], through the random sampling (Monte Carlo sampling method) 10000 times, 10000 samples of pipeline condition parameters can be obtained. Thus, through inputting these samples into these functions in Matlab, how many times the result is larger than σ_a (allowable yield) can be obtained and the pipeline failure probability can be obtained through the time dividing 10000.

2.7. The workflow of the methodology

Fig. 1 shows the methodology of this study. For clarification of input data, output data, used tool, and workflow, Fig. 6 shows the detailed workflow of methodology. All tools mentioned above are shown in this figure, for obtaining the tensile stress and the pipeline failure, the workflow uses AutoFusion, OpenFOAM, Paraview, and a modified pipeline mechanical model with the calculation space, pipeline, and debris flow parameters. The workflow also responds to the content of this section.

3. Application of this study

3.1. Basic assumption and preprocessing

The primary aim of this study is to establish a methodology for assessing oil pipeline failure probability instead of reconstructing historical pipeline failure accidents caused by debris flow. While setting the debris flow initial conditions and pipeline alignment, the situation of debris flow and pipeline based on history and reality should be taken into account. As known, debris flows can occur in steep mountains, e.g., those in Hong Kong [21]. Moore, Lee, and Hencher described a steep catchment (slopes of 35°–40°) on the northern slopes of Lantau Island, east of Tung Chung, Hong Kong, which resulted in a high probability of debris flow by rainstorms. Moreover, the debris flow source might be due to blockage, which triggers the formation of a natural dam, e.g., the Mocoa debris flow in 2017 [20] and the Honduras debris flow in 1934 [23]. Once the dam collapses over a short period, the mass can achieve a high

Table 1
Parameters for calculating oil pipeline failure probability.

Parameter	Mean/uniform value	Coefficient of variation
E Modulus of elasticity	201 MPa	–
v Poisson's ratio	3.425	–
P internal pressure	5 MPa	0.1
r radius of pipeline	0.175	–
t temperature	10 °C	0.15
a coefficient	$11.7*10^{-6}$ °C	–
w pipe wall thickness	7.92 mm	
Internal diameter	31.2 cm	
Allowable stress σa = 0.6*σy	300 MPa	

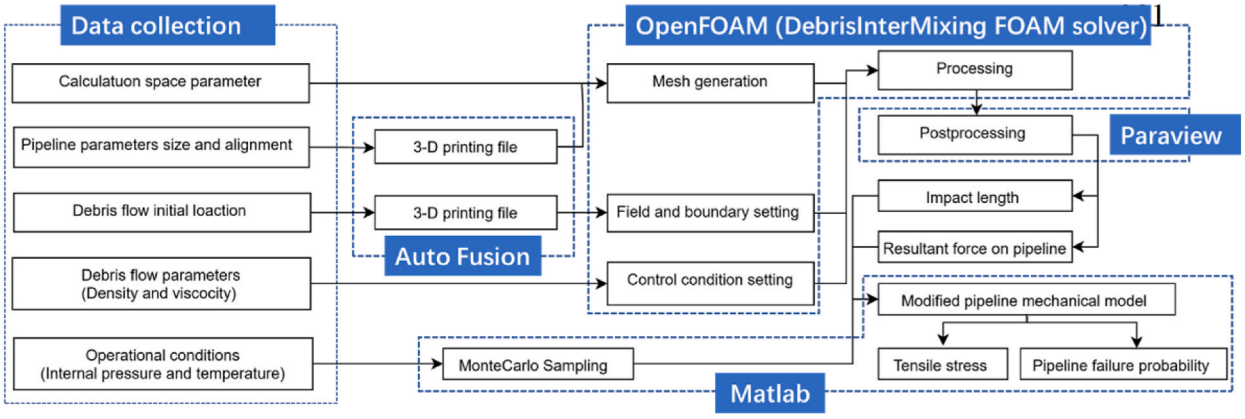

Fig. 6. The detailed workflow of the methodology.

velocity, which results in severe consequences. This study investigating the debris flow scenarios can improve our understanding of the two abovementioned debris flows. Thus, the initial debris flow source was shaped as a regular cube (5 m × 5 m × 4 m) with a regular soil layer.

On the horizontal plane, Fig. 7 shows the bird's eye view map of the debris flow source which is located on a 45° slope at the center of the boundary of calculation space (sited as 25 m × 25 m × 4 m). For clarifying pipeline routes scenarios, following the above description, a line is sited crossing the center of the source and the calculation space, which is shown in Fig. 7. Points on the line can be the origin to determine the pipeline routes.

There are countless possible pipelines crossing an origin. For the simplification and observation of the characteristics of the different-route pipeline, this study only chooses representative pipeline routes through the combination between three origins and three angles. As shown in Fig. 7, point A, B, and C is 5 m, 10 m, and 15 m from point O on the dash line. For each point, three lines are sited crossing the point and of 30°, 60°, and 90° with the dash line. In the vertical direction, the oil pipeline lain-out method is set as one type of aboveground pipeline, surface laid pipeline. In this study, Alvarano-Franco et al. present a quantitative-mechanistic model for assessing the probability of pipeline failures due to the landslide and applied the proposed method to the pipelines network of Colombia [25]. Parameters for calculating oil pipeline failure probability are shown in Table 1. Fig. 8 shows the preprocessing of simulation in OpenFOAM including the mesh generation and field setting.

3.2. Result and discussion

3.2.1. Debris flow movement process

When the mass begins to shift, the gravitational potential energy begins to be converted into kinetic energy. Initially, the mass located at the same inflow plane begins to flow with an initial velocity of 0 m/s along the x- and y-axis directions. Owing to the transformation from gravitational potential energy to kinetic energy, the mass that still flows along the slope obtains its velocity only along the x-axis direction. In the y-axis direction, the mass remains at a velocity of 0 m/s owing to the blocking effect of the channel wall until it flows out from the inflow. Thus, for the unit mass, the blocking effect of the channel wall delays the increase in the y-axis

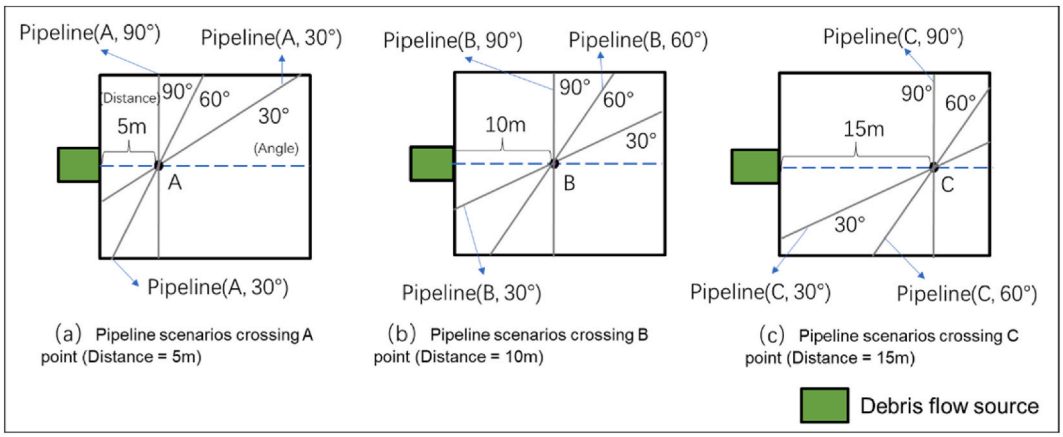

Fig. 7. Pipeline scenarios in this study.

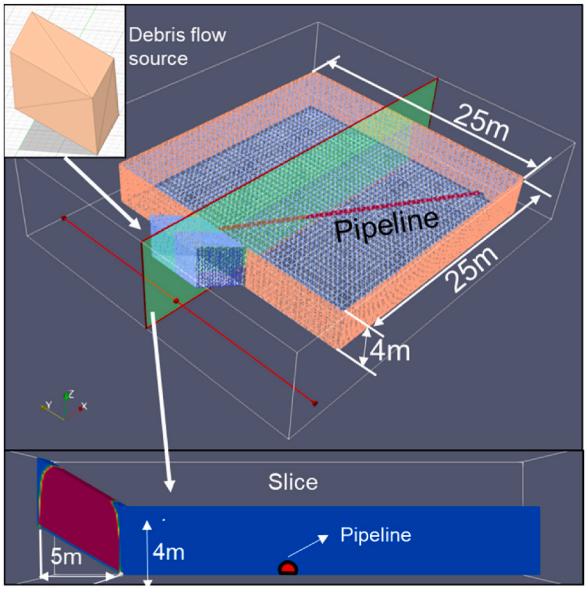

Fig. 8. Preprocessing of simulation in ParaView.

velocity, not in the x-axis velocity, which results in a fan-shaped debris flow. Fig. 9 shows the spatial distribution of the slurry proportion in each cell in the calculation space. The red region, which shows the debris flow process, indicates that the debris flow masses occupy the cells. As mentioned above, debris flow can be regarded as a type of fluid. According to Bernoulli's law, the total pressure of a fluid comprises static and dynamic pressures, which is also known as stagnation pressure. Generally, when a fluid impacts a solid,

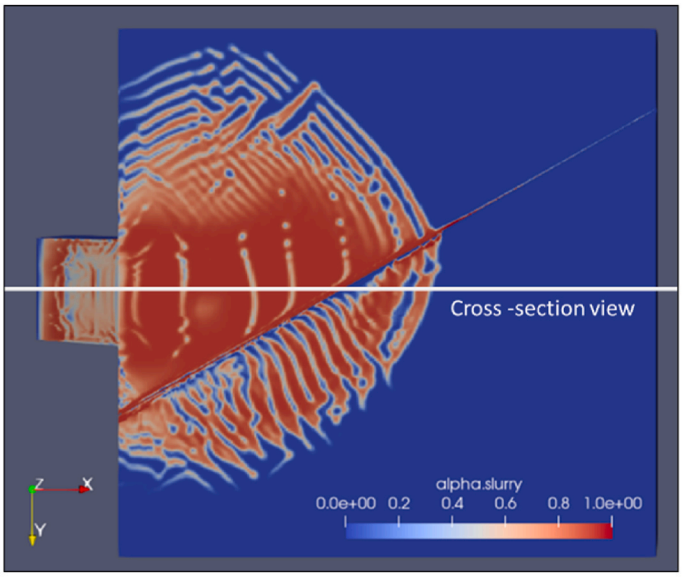

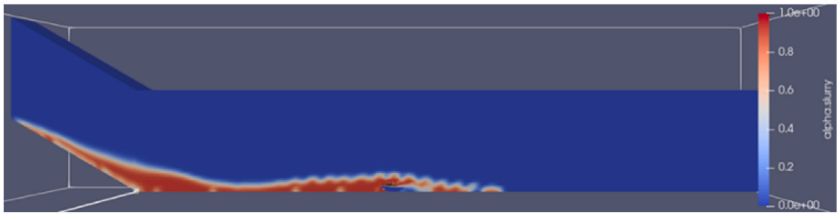

Fig. 9. Debris flow simulation (5 m, 30°) in ParaView (bottle and cross-section views).

stagnation pressure forms at the solid surface. In this study, at the beginning of the impact of debris flow on the pipeline surface, stagnation pressure forms at one side of the pipeline surface, which is the primary contributor to the shape change of the pipeline. Over time, the debris flow overtops the pipeline surface, and stagnation pressure continues to be generated on one side, whereas static pressure starts to be generated on the other side of the pipeline surface. Thus, because of the balance between the two sides of the pipeline, the dynamic pressure becomes the main contributor to the shape changes of the pipeline.

As explained in this section, in the spatial dimension, the different velocities of debris flow in the calculation space cause the fan-shape disposition and the different dynamic pressure on the pipeline surface. In addition, in the temporal dimension, the impacted length, and the velocity on the cells of the grid is changing over time. These changes can cause a change of the resultant force on pipelines, tensile stress, and the pipeline failure probabilities over time.

3.2.2. The impacted length and resultant force on pipelines

During the beginning 4-s period, the impact length started to increase gradually to the pipeline maximum length. Owing to the fan shape characteristic of the debris flow deposition, the impact process is uncertain due to the irregular deposition shape. Different initial conditions of debris flow and pipeline can cause different impact processes for different cases. Fig. 11 show the effect of changing the impacted length of the different pipeline routes. Fig. 11–1 shows that Pipeline (A, 30°) is the first impacted by debris flow and the impacted length on Pipeline (A, 30°) has a more moderate rate of increase than on Pipeline (A, 60°) and Pipeline (A, 90°). As shown in Fig. 7, Pipeline (A, 30°), Pipeline (A, 60°) and Pipeline (A, 90°) have the same origin and when the value along the x-axis is determined, Pipeline (A, 30°) has the smallest value along the y-axis and lead to the shortest reaching time along the three-angles pipelines when facing the same debris flow scenario. Because of the limitation of calculation space, the lengths of pipelines are different, which leads to differences in the period of reaching the maximum length. But Fig. 7 shows that the pipeline (A, 90°) is of the shortest length, and debris flow reaches the maximum pipeline length fastest. This is mainly due to the angle difference of pipelines. In this calculation space, as the debris flow locates at the center of the boundary, the distance between the debris flow and the boundary along the Y-axis is half of the distance along the X-axis. It means that the debris flow arrives at the X-axis boundary first and more time is spent on flowing to Y axis boundary. The length of Pipeline (A, 90°) along the X-axis is equal to only the diameters, while Pipeline (A, 60°) and pipeline (A, 30°) have more length along the X-axis. Thus, when Pipeline (A, 90°) is impacted totally (along X-axis and Y-axis), Pipeline (A, 60°) and Pipeline (A, 30°) can be impacted partly along the X-axis. Pipelines of the origin B and C have the same behavior.

Besides the impacted length, the pipeline failure status is determined by the resultant force on the pipeline. Fig. 12 (1–3) show the variation in the resultant impact force over time on the different-route pipeline. All the curves exhibit the same trend, i.e., increasing and then decreasing as the variation of the velocities. Considering the peak value of every location, the high peak values of the total resultant force on the pipeline (60°, B) and pipeline (60°, C) and the values were approximately pipeline (90°, B) and pipeline (90°, C) separately. While for the pipelines that cross the A point, the resultant force on the pipeline (90°, A) is larger than the pipeline (30°, A) and pipeline (60°, A). In this study, the viscosity of the debris flow-induced tensile stress on the pipeline is ignored. In the x–y plane, the pipelines of 90° are primarily affected by the force along the X-axis, and due to the angle (30° and 60°), the pipeline is affected by the forces along the Y- and X-axis. For most of the mass units, the gravitational potential energy is primarily converted into kinetic energy and the velocity direction is along the X-axis before the mass flows out of the inflow, which causes the velocity along the Y-axis to exceed that along the X-axis. The load on the pipeline is determined by the velocity components perpendicular to the pipeline of velocities along the Y- and X-axis as shown in Fig. 10. For clarifying the importance of angle, Fig. 10 uses the Cartesian coordinate system to discuss the velocity distribution on the pipeline. When the angle is equal to 45°, the velocities along the Y- and X-axis contributing to the velocity components perpendicular to the pipeline have the same weight. As the angle exceeds 45°, the weight of the velocity along the X-axis is larger than Y-axis and when lower than 45°, the weight is smaller than Y-axis. As mentioned above, during the process the velocity along the X-axis is larger than the Y-axis. Thus, when the angle is 30°, the resultant force is lower than that when the angle is equal 60° and 90°.

When the angles are the 60° and 90°, the resultant forces are closed, or the force value on the 60° pipeline is lower than that of the 90° pipeline. Before the debris flow covers the maximum length of the pipeline, the pipeline already is impacted by the peak of the total resultant force. This means that the limitation of pipeline length is excluded. For pipelines crossing the point B and C, such as pipeline (B, 60°) and pipeline (B, 90°), the contribution of velocities along the X-axis to pipeline (B, 90°) is a little larger than the pipeline (B, 60°). However, the velocity along the Y-axis compensates for this difference. For pipelines crossing point A, due to the short straight

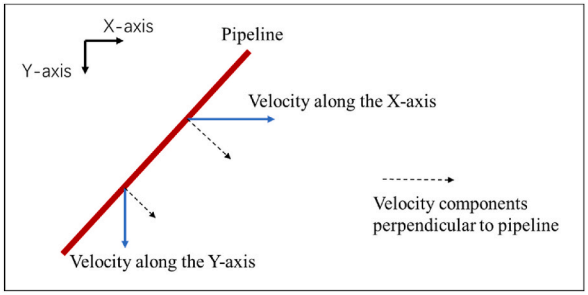

Fig. 10. Velocity distribution on the pipeline.

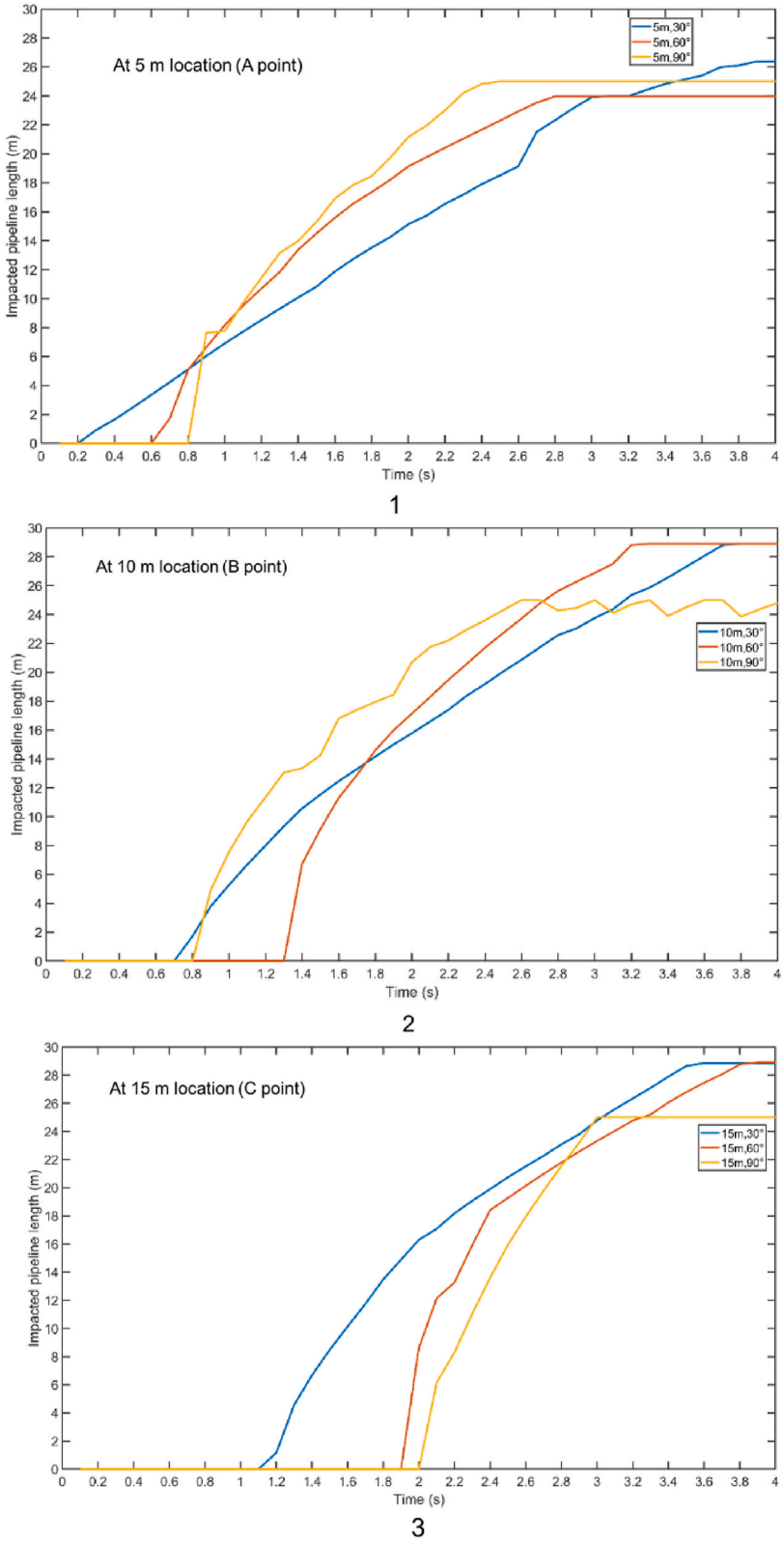

Fig. 11. Impacted pipeline length vs. time.

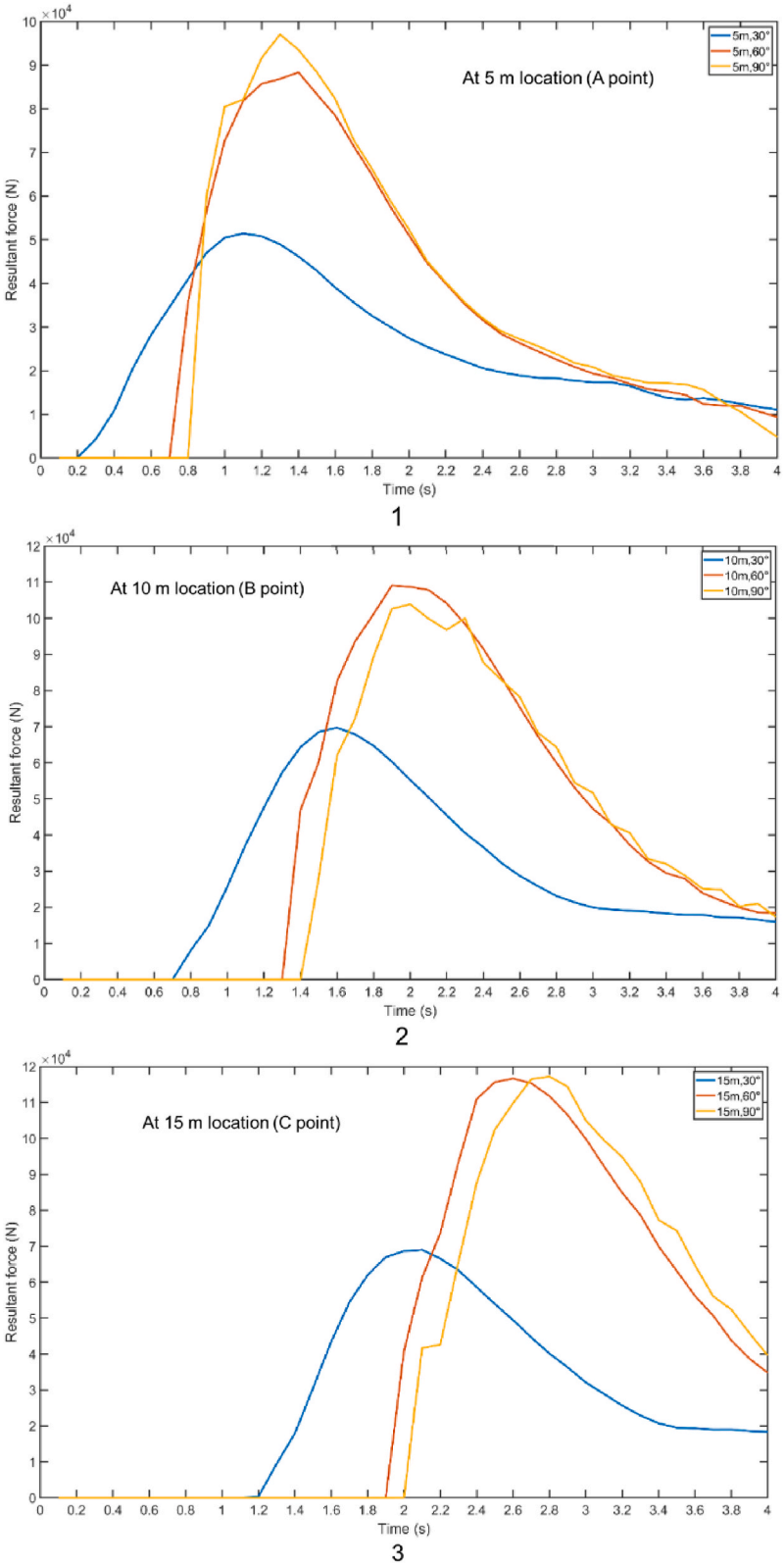

Fig. 12. Impacted pipeline length vs. time.

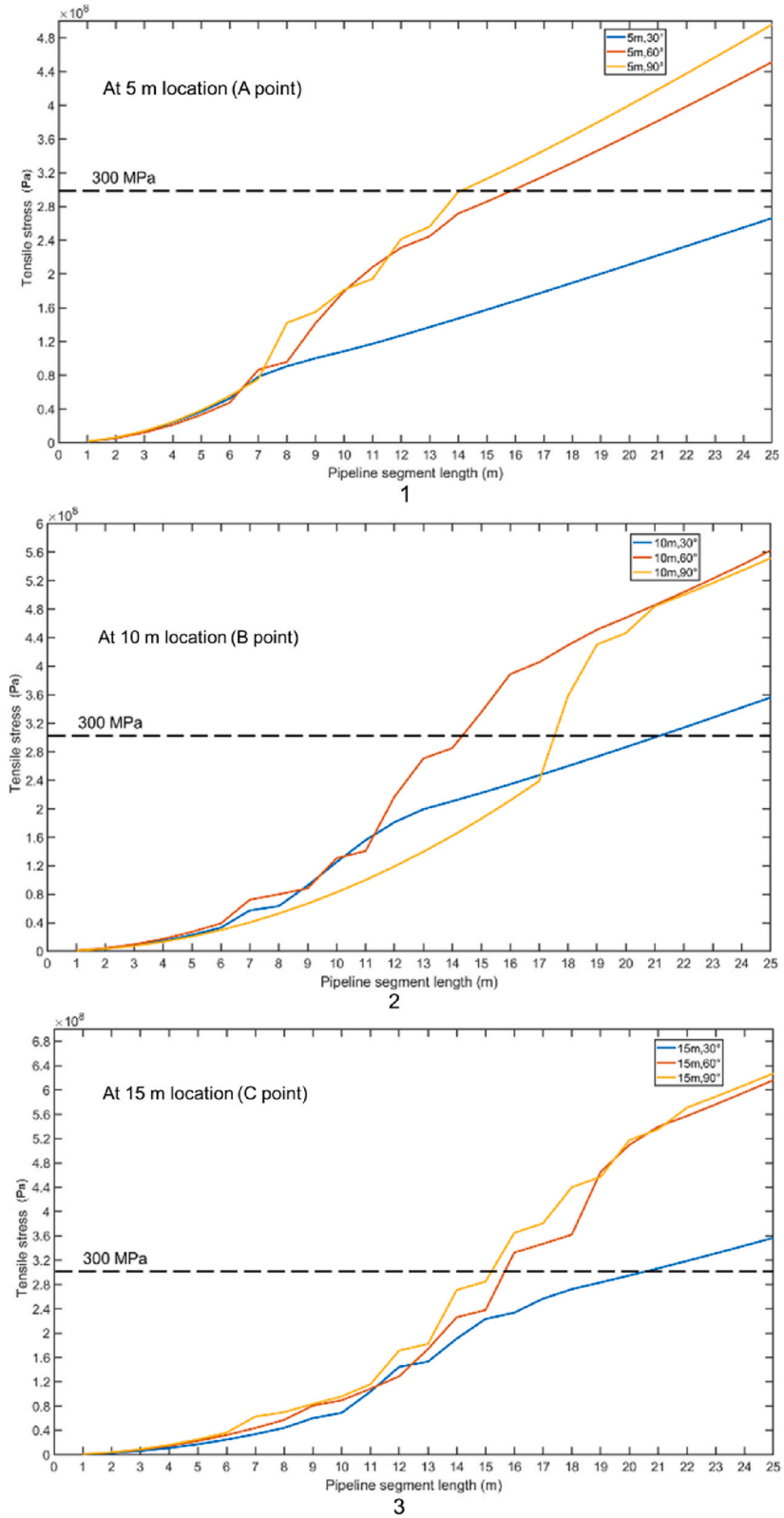

Fig. 13. Tensile stress vs. segment length.

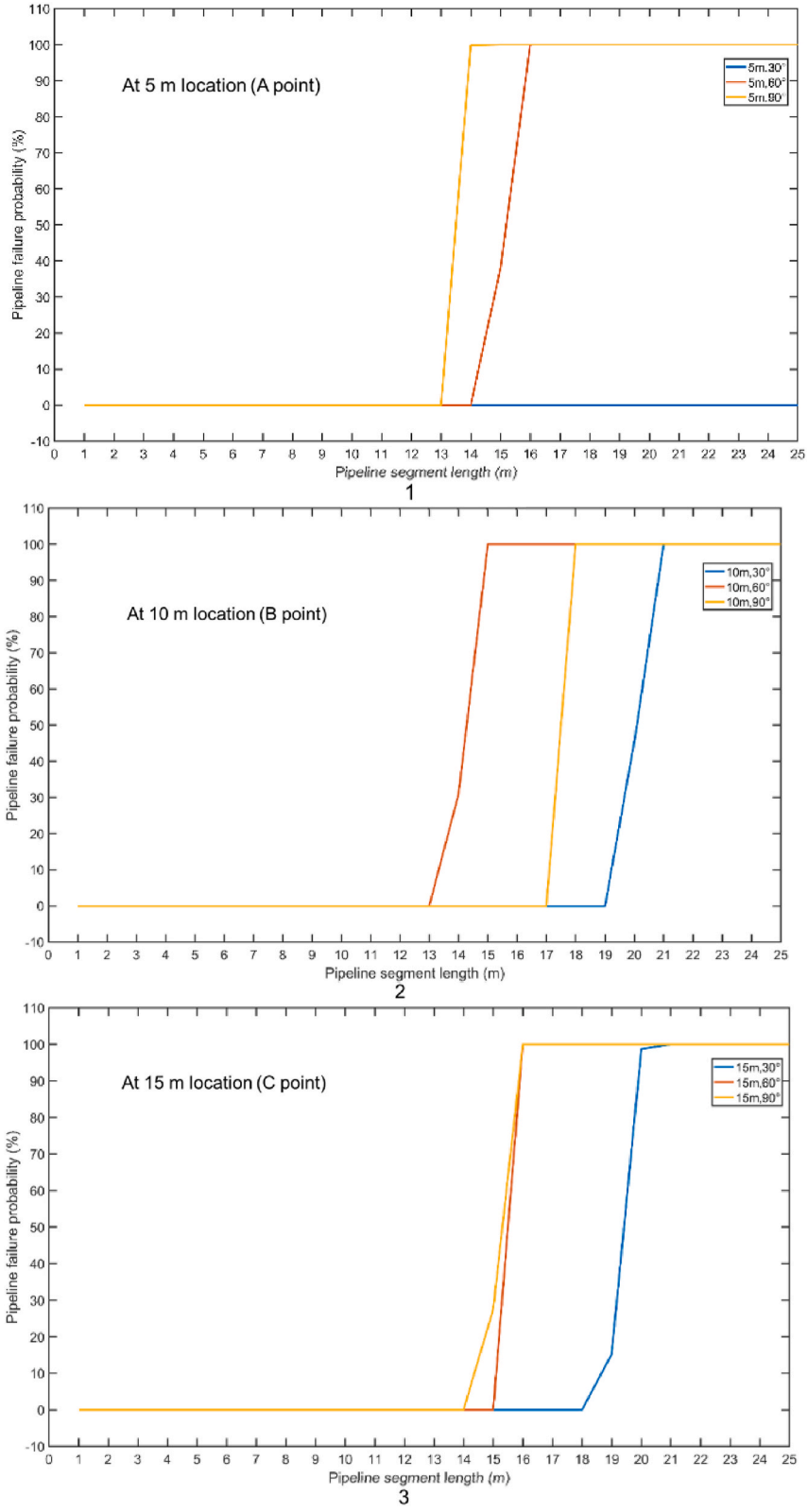

Fig. 14. Pipeline failure probability vs. segment length.

distance between the center of the boundary and the point, along the Y-axis, the debris flow does not obtain enough velocity, and the velocity components perpendicular to the pipeline are sensitive to the angle.

In addition, comparing the resultant force of the same angle at different positions, the force was lower at positions closer to the outflow of debris flow. In this subsection, although the resultant forces are described based on basic mechanical assumptions, they cannot be used as the final proof for the pipeline protection measures because the pipeline failure is caused by the joint action at different locations.

3.2.3. Calculation of tensile stresses due to debris flow

Fig. 13 (1)–(3) show the increase in tensile stresses along with the increase in the pipeline segment length with the maximum resultant force during the flow period. All the curves show that as the pipeline segment length increased, the stress continued to increase. In Fig. 13 (1–3), at every location, the stress of the pipelines of 30° remained the lowest value as the segment length increased. Figs. 13–1 shows the results for the pipelines using A point as the origin. The stress of pipeline (A, 90°) was the highest, followed by those at pipeline (A, 60°) and pipeline (A, 30°). Figs. 13–2 shows the results for the pipelines using B point as the origin. The pipeline (B, 90°) indicated volatility as the segment length increased, and the 17 m segment length was the threshold. When the segment length was shorter than 17 m, the tensile stress of the 90° pipeline was the lowest. For pipelines longer than 17 m, the tensile stresses of the 90° pipeline increased and approached the value of the 60° pipeline. Figs. 13–3 shows that the tensile stresses at the C point position exhibited a similar tendency to those at the A point position. Notably, the tensile stresses of the pipeline (C, 60°) and pipeline (C, 90°) were similar. In addition, the tensile stress curve shows the effects of the impacted and segment lengths. Because the maximum resultant force is used without considering the impacted length, the maximum resultant force is positively correlated with the tensile stress under the same segment length. Owing to the uncertainties of the impacted and segment lengths, pipeline (B, 60°) shows a characteristic of volatility. This furtherly demonstrates the importance of considering the segment and impacted lengths simultaneously, examining the change in the impacted length, and understanding the debris flow process.

The tensile stress can be used as a reference for decision-making as well as to determine pipeline failure. The operating conditions can increase the total stress. If the normal stress exceeds the allowable equivalent stress, then even if the operating condition exists, the pipeline will likely fail. Notably, the force along the z-axis is the difference between the lift force owing to debris flow and the gravitational force owing to the oil and pipeline. The normal stress considers the gravitational impact of the oil on the z-axis, as well as the operating conditions. While the lack of pipeline operational data, the normal stress can supply criteria to determine the pipeline is safe or fail.

3.2.4. Pipeline failure probability

Regarding the pipeline failure probability due to the uncertainty of the operation conditions, the probability increased from 0 to 1 for each position when the strength was set to 300 MPa (σ_a). Fig. 14 (1–3) shows that most of the curves exhibited the same trend, i.e., beginning at 0, followed by increasing from 0 to 1, and then maintaining at 1 as the segment length increased. The pipeline (A, 30°) remained safe as the segment length increased owing to the low resultant force. For most curves, the pipeline failure probability from 0 to 1 was located over different ranges of the pipeline segment lengths. For example, for pipeline (A, 90°), the range was from 13 to 14 m. For pipeline (B, 90°), the range was from 13 to 15 m.

The pipeline failure curve shows an increase in the probability from 0 to 1. Different pipeline alignments have different allowable maximum segment lengths for ensuring pipeline safety. When the probability reaches 0, the uncertainty of the operating conditions does not affect the probability under the same segment length. While the probability reaches 1, the appropriate measures should be implemented urgently. In some situations, the uncertainty of the operating conditions does not affect the probability. During the life cycle of the pipeline, the pipeline segment should be lower than the maximum allowable pipeline segment length by local authorities and stakeholders. For an existing pipeline, the operators of the pipeline should be aware of the pipeline failure probability and implement the necessary measures to reduce the probability, such as by adding barriers to decrease the segment length.

4. Conclusion and limitations

This study provides basic information regarding the layout of pipelines, the probability of damage to pipelines, and the maximum length of pipeline sections based on the operating conditions of pipelines. In this study, the pipelines of 30° the tensile stress has a more moderate increase rate with the increase of pipeline segment length, for the pipelines of 60° and 90°, at 5 m and 15 m locations they have a similar increase rate and value, but at 10 m location, the pipelines of 60° shows the volatile characteristic. Also, the pipeline failure probability of 30° keeps 0 at the 5-m location, other pipelines show the same trend from 0 to 1. At 5 m and 15 m locations, the failure probabilities of the pipelines of 60° and 90° start to increase when the segment length is 13–14 m, while for other pipelines the segment length is 17–19 m as shown in Table 4. Moreover, Table 2 shows the maximum resultant force on pipelines and Table 3 shows the maximum tensile stress of pipelines. These information can be provided to local authorities, stakeholders, and operators for decision-making during the lifecycle of pipelines, i.e., during the construction, operation, and maintenance stages. Furthermore, these information can be used to generate a pipeline failure map for providing visual guidance. The importance of the impacted pipeline length at different locations and angles was clarified in this study, where different effects on the normal stress were demonstrated. Furthermore, this indicates the necessity for a pipeline mechanical model.

Fig. 7 shows the workflow of the methodology, there are limitations at each step of the application. This study aims to propose a methodology to solve the practice problem. However, the limitation involved in this study should be clarified. During the data collection, this study uses the literature data from Von Boetticher et al.'s research [12] and Ahammed M et al.'s [10]. In the real world,

Table 2
The maximum resultant force on pipelines.

Degree Distance	30°	60°	90°
5 m	51446.1	88337.9	97065.8
10 m	69731.4	109082.4	103909.6
15 m	69012.2	116685.7	117239.7

Table 3
The maximum tensile stress of pipelines.

Degree Distance	30°	60°	90°
5 m	266 MPa	451 MPa	496 MPa
10 m	356 MPa	562 MPa	551 MPa
15 m	357 MPa	616 MPa	627 MPa

Table 4
The maximum segment length for keeping the pipeline safe.

Degree Distance	30°	60°	90°
5 m	–	14 m	13 m
10 m	19 m	13 m	17 m
15 m	18 m	15 m	14 m

the triggering and fluid process of a debris flow can be more comprehensive and pipeline structure and operating conditions are more complex. The models need to be verified using the site data. Moreover, during the preprocessing, due to the calculation capacity, the debris flow source is small but it spent one day on calculation for one time. Furthermore, when calculating the tensile stress and pipeline failure probability, the simplified beam model applied in this study assumes that pipe loading by debris flow is uniform; however, in practice, this results in stress concentrations. At positions closer to the midline, loading becomes greater owing to the viscous nature of debris flow. When an inundated area is larger than the pipe length, the results may be underestimated.

Author contribution statement

Su SONG: Conceived and designed the experiments; Performed the experiments; Analyzed and interpreted the data; Wrote the paper.

Weizhuo HUA: Conceived and designed the experiments; Performed the experiments.

Xiaolong LUO: Conceived and designed the experiments.

Ana Maria CRUZ: Conceived and designed the experiments; Contributed reagents, materials, analysis tools or data; Wrote the paper.

Data availability statement

Data will be made available on request.

Declaration of competing interest

The authors declare that they have no known competing financial interests or personal relationships that could have appeared to influence the work reported in this paper.

Acknowledgements

This research was supported by the Japan Society for the Promotion of Science, [Kaken Grant 17K01336, April 2017–March 2020] and [Kaken Grant 19H00809, April 2019–March 2022] as well as Kyoto University Research Development Program (ISHIZUE 2021).

References

[1] E. Krausmann, A.M. Cruz, E. Salzano, Natech Risk Assessment and Management: Reducing the Risk of Natural-Hazard Impact on Hazardous Installations, Elsevier, 2017.

[2] A.M. Cruz, L.J. Steinberg, A.L. Vetere Arellano, J.-P. Nordvik, F. Pisano, State of the Art in Natech Risk Management, 2004.

[3] J.W. Kean, D.M. Staley, J.T. Lancaster, F.K. Rengers, B.J. Swanson, J.A. Coe, et al., Inundation, flow dynamics, and damage in the 9 January 2018 Montecito debris-flow event, California, USA: opportunities and challenges for post-wildfire risk assessment, Geosphere 15 (2019) 1140–1163, https://doi.org/10.1130/GES02048.1.

[4] S. Girgin, K. Elisabeth, Lessons Learned from Oil Pipeline Natech Accidents and Recommendations for Natech Scenario Development Final Report, 2015, https://doi.org/10.2788/20737.
[5] C-Core, D.G. Honegger Consulting Ssd I, Guidelines for constructing natural gas and liquid hydrocarbon pipelines through areas prone to landslide and subsidence hazards, Des Mater Constr Comm Pipeline Res Counc Int Inc (2009).
[6] A.R. Approach, Transmission Pipelines and Land Use: A Risk-Informed Approach, 2004.
[7] R.S. Read, Pipeline Geohazards: Planning, Design, Construction and Operations, 2019, https://doi.org/10.1115/1.861790.
[8] T. Takahashi, A review of Japanese debris flow research, Int J Eros Control Eng 2 (2009) 1–14, https://doi.org/10.13101/ijece.2.1.
[9] Y. Wu, J. Li, Finite element analysis on mechanical behavior of semi-exposed pipeline subjected to debris flows, Eng. Fail. Anal. 105 (2019) 781–797, https://doi.org/10.1016/j.engfailanal.2019.06.055.
[10] W. Ying, Z. Sixi, J. Pengwei, Finite element method simulations to study factors affecting buried pipeline subjected to debris flow, J Press Vessel Technol Trans ASME 141 (2019), https://doi.org/10.1115/1.4042055.
[11] H. Ma, B. He, X. Luo, W. Cai, D. Liu, C. Hou, et al., Investigation on strain characteristic of buried natural gas pipeline under longitudinal landslide debris flow, J. Nat. Gas Sci. Eng. (2021) 86, https://doi.org/10.1016/j.jngse.2020.103708.
[12] H. Pourziaei Araban, J. Alinejad, M.M. Peiravi, Entropy generation and hybrid fluid-solid-fluid heat transfer in 3D multi-floors enclosure, International Journal of Exergy 37 (3) (2022) 337–355.
[13] M.M. Peiravi, J. Alinejad, 3D numerical simulation of fibers arrangement effects on thermal conductivity of polymer matrix composite, Mech Adv Compos Struct 9 (2022) 59–73, https://doi.org/10.22075/macs.2022.21131.1291.
[14] M.M. Peiravi, J. Alinejad, Nano particles distribution characteristics in multi-phase heat transfer between 3D cubical enclosures mounted obstacles, Alex. Eng. J. 60 (2021) 5025–5038, https://doi.org/10.1016/j.aej.2021.04.013.
[15] J. Alinejad, J.A. Esfahani, Numerical stabilization of three-dimensional turbulent natural convection around isothermal cylinder, J. Thermophys. Heat Tran. 30 (2016) 94–102.
[16] J. Alinejad, J.A. Esfahani, Lattice Boltzmann simulation of a fluid flow around a triangular unit of three isothermal cylinders, J. Appl. Mech. Tech. Phys. 57 (1) (2016) 117–126.
[17] J. Alinejad, N. Montazerin, S. Samarbakhsh, Accretion of the efficiency of a forward-curved centrifugal fan by modification of the rotor geometry: computational and experimental study, J Fluid Mech Res 40 (6) (2013) 469–481.
[18] R.L. Baum, D.L. Galloway, E.L. Harp, Landslide and land subsidence hazards to pipelines, Open File Rep. 1164 (2008) 192.
[19] M. Ahammed, R.E. Melchers, Probabilistic analysis of underground pipelines subject to combined stresses and corrosion, Eng. Struct. 19 (1997) 988–994, https://doi.org/10.1016/S0141-0296(97)00043-6.
[20] L. Rossi, V. Casson Moreno, G. Landucci, Vulnerability assessment of process pipelines affected by flood events, Reliab. Eng. Syst. Saf. 219 (2022), 108261, https://doi.org/10.1016/j.ress.2021.108261.
[21] A Von Boetticher, DebrisInterMixing-2.3: a Finite Volume solver for three dimensional debris flow simulations based on a single calibration parameter – Part 1: model description, Geosci. Model Dev. Discuss. (GMDD) 8 (2015) 6349–6378, https://doi.org/10.5194/gmdd-8-6349-2015.
[22] A. Von Boetticher, J.M. Turowski, B.W. McArdell, D. Rickenmann, M. Hürlimann, C. Scheidl, et al., DebrisInterMixing-2.3: a finite volume solver for three-dimensional debris-flow simulations with two calibration parameters - Part 2: model validation with experiments, Geosci. Model Dev. (GMD) 10 (2017) 3963–3978, https://doi.org/10.5194/gmd-10-3963-2017.
[23] A. Von Boetticher, J.M. Turowski, B.W. McArdell, D. Rickenmann, J.W. Kirchner, DebrisInterMixing-2.3: a finite volume solver for three-dimensional debris-flow simulations with two calibration parameters - Part 1: model description, Geosci. Model Dev. (GMD) 9 (2016) 2909–2923, https://doi.org/10.5194/gmd-9-2909-2016.
[24] The Standardization Administration of the People's Republic of China, Code for Design of Oil Transportation Pipeline Engineering, 2014.
[25] J.P. Alvarado-Franco, D. Castro, N. Estrada, B. Caicedo, M. Sánchez-Silva, L.A. Camacho, F. Muñoz, Quantitative-mechanistic model for assessing landslide probability and pipeline failure probability due to landslides, Eng. Geol. 222 (2017) 212–224.